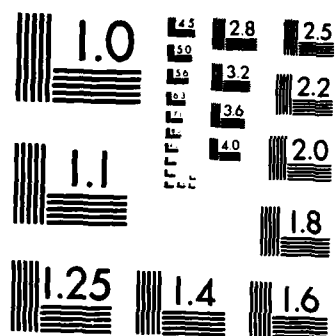


RESONANCE FLUORESCENCE OF A TWO-LEVEL ATOM NEAR A ROUGH  
METAL SURFACE (U) STATE UNIV OF NEW YORK AT BUFFALO  
DEPT OF CHEMISTRY X HUANG ET AL JAN 86

UROCHESTER/DC/85/TR-4 N00014-86-K-0043

F/G 7/5

NL



MICROCOPY RESOLUTION TEST CHART  
NATIONAL BUREAU OF STANDARDS-1963-A

AD-A163 219

12

OFFICE OF NAVAL RESEARCH

Contract N00014-86-K-0043

TECHNICAL REPORT No. 4

Resonance Fluorescence of a Two-Level Atom Near a Rough Metal Surface

by

Xi-Yi Huang, Ki-Tung Lee and Thomas F. George

Prepared for Publication

in

Journal of Chemical Physics

Departments of Chemistry and Physics  
State University of New York at Buffalo  
Buffalo, New York 14260

January 1986

Reproduction in whole or in part is permitted for any purpose  
of the United States Government.

This document has been approved for public release and sale;  
its distribution is unlimited.

DTIC FILE COPY

DTIC  
ELECTE  
JAN 21 1986  
S A D

86

1.41

026

UNCLASSIFIED

SECURITY CLASSIFICATION OF THIS PAGE

## REPORT DOCUMENTATION PAGE

1a. REPORT SECURITY CLASSIFICATION Unclassified			1b. RESTRICTIVE MARKINGS		
2a. SECURITY CLASSIFICATION AUTHORITY			3. DISTRIBUTION/AVAILABILITY OF REPORT Approved for public release; distribution unlimited		
2b. DECLASSIFICATION/DOWNGRADING SCHEDULE					
4. PERFORMING ORGANIZATION REPORT NUMBER(S)  UBUFFALO/DC/85/TR-4			5. MONITORING ORGANIZATION REPORT NUMBER(S)		
6a. NAME OF PERFORMING ORGANIZATION Depts. Chemistry & Physics State University of New York		6b. OFFICE SYMBOL (If applicable)		7a. NAME OF MONITORING ORGANIZATION	
6c. ADDRESS (City, State and ZIP Code) Fronczak Hall, Amherst Campus Buffalo, New York 14260		7b. ADDRESS (City, State and ZIP Code) Chemistry Program 800 N. Quincy Street Arlington, Virginia 22217			
8a. NAME OF FUNDING/SPONSORING ORGANIZATION Office of Naval Research		8b. OFFICE SYMBOL (If applicable)		9. PROCUREMENT INSTRUMENT IDENTIFICATION NUMBER Contract N00014-86-K-0043	
8c. ADDRESS (City, State and ZIP Code) Chemistry Program 800 N. Quincy Street Arlington, Virginia 22217		10. SOURCE OF FUNDING NOS.			
		PROGRAM ELEMENT NO.		PROJECT NO.	TASK NO.
					WORK UNIT NO.
11. TITLE Resonance Fluorescence of a Two-Level Atom Near a Rough Metal Surface					
12. PERSONAL AUTHOR(S) Xi-Yi Huang, Ki-Tung Lee and Thomas F. George					
13a. TYPE OF REPORT Interim Technical		13b. TIME COVERED FROM _____ TO _____		14. DATE OF REPORT (Yr., Mo., Day) January 1986	
15. PAGE COUNT 24					
16. SUPPLEMENTARY NOTATION Prepared for publication in the Journal of Chemical Physics					
17. COSATI CODES			18. SUBJECT TERMS (Continue on reverse if necessary and identify by block number)		
FIELD	GROUP	SUB. GR.	RESONANCE FLUORESCENCE		
			TWO-LEVEL ATOM		
			LASER DRIVEN		
			SURFACE DRESSED		
			ROUGH METAL SURFACE		
			ADATOM+HEMISPHEROID		
19. ABSTRACT (Continue on reverse if necessary and identify by block number)  Surface-dressed optical Bloch equations are solved for a two-level atom near or adsorbed on a rough surface, which is modeled as a hemispheroid protrusion on a perfectly-conducting surface. Effects of the laser bandwidth are included by means of a phase-diffusion model. The presence of the surface roughness generates a dephasing broadening mechanism on the adatomic resonance fluorescence spectrum, which can be strongly enhanced by plasmon resonances depending on the shape of the hemispheroid. The dependence of the electrodynamics of the adatom on the adatom-hemispheroid distance is also evaluated. <i>Keywords:</i>					
20. DISTRIBUTION/AVAILABILITY OF ABSTRACT UNCLASSIFIED/UNLIMITED <input checked="" type="checkbox"/> SAME AS RPT. <input checked="" type="checkbox"/> DTIC USERS <input type="checkbox"/>			21. ABSTRACT SECURITY CLASSIFICATION Unclassified		
22a. NAME OF RESPONSIBLE INDIVIDUAL Dr. David L. Nelson			22b. TELEPHONE NUMBER (Include Area Code) (202)696-4410		22c. OFFICE SYMBOL

DD FORM 1473, 83 APR

ON OF 1 JAN 73 IS OBSOLETE.

UNCLASSIFIED

SECURITY CLASSIFICATION OF THIS PAGE

Resonance Fluorescence of a Two-Level Atom Near a Rough Metal Surface

Xi-Yi Huang

Department of Chemistry  
University of Rochester  
Rochester, New York 14620

Ki-Tung Lee

Department of Chemistry  
Illinois Institute of Technology  
Chicago, Illinois 60616

Thomas F. George

Departments of Chemistry and Physics  
State University of New York at Buffalo  
Buffalo, New York 14260

Abstract

Surface-dressed optical Bloch equations are solved for a two-level atom near or adsorbed on a rough surface, which is modeled as a hemispheroid protrusion on a perfectly-conducting surface. Effects of the laser bandwidth are included by means of a phase-diffusion model. The presence of the surface roughness generates a dephasing broadening mechanism on the adatomic resonance fluorescence spectrum, which can be strongly enhanced by plasmon resonances depending on the shape of the hemispheroid. The dependence of the electrodynamics of the adatom on the adatom-hemispheroid distance is also evaluated.

Author	
RA&I	<input checked="" type="checkbox"/>
B	<input type="checkbox"/>
Indexed	<input type="checkbox"/>
Title	
Abstract	
Distribution	
Applied	
Dist	
A-1	

## 1. Introduction

There is considerable interest in the interaction of laser radiation with adspecies on surfaces.<sup>1</sup> In particular, researchers have studied the problem of surface-enhanced spontaneous emission of two-level atoms near a mirror<sup>2-5</sup> and decay of excited molecules near a small metal sphere.<sup>6</sup> The enhancement of Raman scattering and fluorescence by small metal spheres has also been examined.<sup>7,8</sup> However, when the resonant, driving coherent radiation is very strong, interesting "resonance fluorescence" and other nonlinear phenomena can occur.<sup>9,10</sup> In these cases, the resonant laser puts the atom or molecule in an environment where the probability of stimulated emission can exceed that of spontaneous emission. Under these circumstances we find back-transitions and Rabi oscillations of state probability amplitudes, and the dynamic Stark splitting of resonances and mutational oscillations of the emitted light intensity become important parts of the laser-driving process.<sup>9,10</sup> In a strong resonant field, nonlinear scattering occurs, and multiphoton processes become as important as single-photon processes, so that we can no longer rely on the conventional low-order perturbation theory of fluorescence. In the surface-free case, i.e., in the absence of a solid surface or when the atom is very far from the surface, resonance excitation of a two-level atom by a laser field has been extensively investigated, using the powerful optical Bloch equations.<sup>9,10</sup> Previously, we have derived a set of surface-dressed optical Bloch equations<sup>11-15</sup> by which we can discuss the effects of the surface-reflected photons, the resonance interaction between the adatom and surface-plasmons, the collision dephasing of the adatom produced by gas atoms in the medium, and the random phase fluctuation of the (intense) laser field. In the present paper, we extend the calculation of the resonance fluorescence for a flat-surface<sup>7-8</sup> to the case of an interface with metallic protrusions.

Surface roughness can be characterized as a set of protrusions which randomly (or regularly, in the case of a grating) stick out of the underlying planar substrate. While the protrusions may have different sizes and shapes, in this paper we model the protrusions as a prolate hemispheroid on top of a plane,<sup>16,17</sup> as depicted in Fig. 1. We note that the model of a half spheroid on a flat perfect conductor<sup>16</sup> has been shown to be identical to a full spheroid in a vacuum.<sup>1b</sup> Thus the following discussion can be also used for ellipsoidal cases. The two-level adatom, which is located at a distance  $d$  from the top of the hemispheroid, is driven by a laser. The adatom has no dipole moment in its ground state, but it can have a transition dipole connecting the ground and excited states. The emitted photons will be reflected by the flat mirror and the hemispheroid, which in turn provide a resonance feedback to the dynamics of the adatom. The spectrum of laser light scattering in the presence of a bump-plane surface system near a two-level atom is then the subject of this paper.

## 2. Surface-Dressed Optical Bloch Equations for a Rough Surface

Let us evaluate the light scattering produced when a laser field is incident on a molecule adsorbed on a rough surface. The surface will be taken to be a prolate hemispheroid protruding from a flat plane. The spheroid is assumed to have the complex dielectric constant  $\epsilon(\omega)$ , while the plane is taken to be a perfect conductor. The incident laser field is taken to be propagating along the interface, where its electric field is taken to be along the normal of the interface. The prolated spheroidal coordinate  $(\xi, \eta, \phi)$  system<sup>18</sup> is used to calculate the reflected field. We define

$$\xi_1 = (a + d)/f$$

$$\xi_0 = a/f$$

and

$$f = (a^2 - b^2)^{1/2} ,$$

where  $a$  and  $b$  are the semi-major and semi-minor axes of the hemispheroid (Fig. 1). The reflected field at the position of the adatom (dipole), in the limit of the near-field approximation, can be written as<sup>16</sup>

$$E_r = -\frac{1}{f} \sum_n C_n Q'_n(\xi_1) + \frac{\mu}{4(f\xi_1)^3} \quad (1)$$

where  $Q_n$  denotes the Legendre function of the second kind and  $\mu$  is the induced dipole moment which will be given later. The expansion coefficient  $C_n$  is given by

$$C_n = \frac{(\epsilon - 1)E_0 + \xi_0 \delta_{n,1}}{\epsilon Q_1(\xi_0) - \xi_1 Q'_1(\xi_0)} + \frac{4n + 2}{f^2} \mu \frac{(1 - \epsilon)P'_n(\xi_0)Q'_n(\xi_1)P_n(\xi_0)}{\epsilon Q_n(\xi_0)P'_n(\xi_0) - Q'_n(\xi_0)P_n(\xi_0)} , \quad (2)$$

where  $P_n$  denotes the Legendre function of the first kind and  $E_0$  is the amplitude of the incident laser. The induced dipole moment,  $\mu$ , of the adatom is given by

$$\mu = \alpha E_{\text{total}} ,$$

where  $\alpha$  is the polarizability along the semi-major axis and  $E_{\text{total}}$  is the total



electric field applied to the adatom. The induced dipole moment can be expressed by

$$\mu = \alpha \left( -\frac{1}{f} \sum_n C_n Q'_n(\xi_1) + \frac{\mu}{4(f\xi_1)^3} + E_0 \right) . \quad (3)$$

After rearranging Eq.(3) and substituting back to Eq.(1), we obtain

$$E_r = \frac{E_0}{1 - \Gamma} \left[ \frac{(1 - \epsilon) \xi_0 Q'_1(\xi_1)}{\epsilon Q_1(\xi_0) - \xi_0 Q'_1(\xi_0)} + \Gamma \right] , \quad (4)$$

where

$$\Gamma = \frac{\alpha}{4(f\xi_1)^3} + \frac{2\alpha}{f^3} (\epsilon - 1) \sum_n \frac{(2n + 1) P'_n(\xi_0) [Q_n(\xi_1)]^2 P_n(\xi_0)}{\epsilon Q_n(\xi_0) P'_n(\xi_0) - Q'_n(\xi_0) P_n(\xi_0)} .$$

As shown in Eq.(4), there are two resonance conditions:  $1 - \Gamma$  approaches zero and  $\epsilon$  equals  $\xi_0 Q'_1(\xi_1)/Q_1(\xi_0)$ . It can be shown easily that the near-field approximation will break down when the factor  $1 - \Gamma$  approaches zero. The physical interpretation of this factor is the image enhancement effect. The importance of the image effect has been reviewed by Schatz.<sup>19</sup> Let us focus on the second resonance condition. We recall that

$$Q_1(\xi) = \frac{\xi}{2} \ln \left[ \frac{\xi + 1}{\xi - 1} \right] - 1 .$$

Hence, we can write the second resonance condition as

$$\epsilon = \frac{(\xi_0/2) \ln[(\xi_0 + 1)/(\xi_0 - 1)] - \xi_0^2/(\xi_0^2 - 1)}{(\xi_0/2) \ln[(\xi_0 + 1)/(\xi_0 - 1)] - 1} . \quad (5)$$

Using the identity

$$(\xi^2 - 1)^{-1} = \sum_n \xi^{-2n}$$

we obtain

$$\epsilon = 1 - \frac{1}{Q_1(\xi_0)(\xi_0^2 - 1)} . \quad (6)$$

In the limit  $\xi_0 \rightarrow \infty$  such that the spheroid tends towards a sphere, Eq.(6)

becomes

$$\epsilon(\xi_0 \rightarrow \infty) = 1 - \frac{3\xi_0^2}{\xi_0^2 - 1} \approx -2, \quad (7)$$

which reduces to the usual surface plasmon resonance condition of a sphere,  $\epsilon + 2 = 0$ . We will discuss below how to use this reflected field to calculate the transition dipole.

To treat problems of excitation and dissipation of a two-level adatom near a hemispheroid, a self-consistent approach is developed in which the dynamical behavior associated with the induced transition dipole is determined by surface dressed optical Bloch equations (SBE).<sup>11,12</sup> Essentially, the SBE are quantum operator equations for  $\hat{\sigma}_{12}$ ,  $\hat{\sigma}_{21}$  and  $\hat{W}$ , where  $\hat{\sigma}_{ij} = |i\rangle\langle j|$  ( $i, j = 1, 2$ ) are the adatomic transition operators and  $\hat{W}(t) = \hat{\sigma}_{22}(t) - \hat{\sigma}_{11}(t)$  is the population inversion of the adatom. By defining

$$\hat{S}_{12}(t) = \hat{\sigma}_{12}(t) \exp(i\omega_L t) \quad (8)$$

$$\hat{S}_{21}(t) = \hat{\sigma}_{21}(t) \exp(-i\omega_L t) \quad (9)$$

where  $\omega_L$  is the laser frequency, we can write the rotating-wave approximation (RWA) for the SBE of the adatom-bump system as

$$\frac{d}{dt} \begin{bmatrix} \hat{S}_{21}(t) \\ \hat{W}(t) \\ \hat{S}_{12}(t) \end{bmatrix} = \begin{bmatrix} -\tilde{\gamma}_2 + i\Delta & \frac{i\Omega^-(t)}{2} & 0 \\ i\Omega^+(t) & -\gamma_1 & -i\Omega^-(t) \\ 0 & \frac{-\Omega^+(t)}{2} & -\tilde{\gamma}_2 - i\Delta \end{bmatrix} \begin{bmatrix} \hat{S}_{21}(t) \\ \hat{W}(t) \\ \hat{S}_{12}(t) \end{bmatrix} - \gamma_1 \begin{bmatrix} 0 \\ 1 \\ 0 \end{bmatrix}.$$

$\Omega^\pm(t) = \Omega \exp[\mp i\phi(t)]$  is the time-dependent Rabi frequency, where

$\Omega = (2/\hbar) |\mu_{21}| E_0(t)$  and  $E(t)$  is written as an expectation value in a coherent state of the laser field in terms of the phase factor  $\phi(t)$  as

$E(t) = E_0(t) \exp[-i\omega_L t + i\phi(t)] + \text{c.c.}$ ;  $\Delta = \omega_{21} - \omega_L$  is the detuning; the surface-induced phase-decay  $\tilde{\gamma}_2 = \gamma_2 + \gamma_s$ , where  $\gamma_s$  is determined by the

reflected field which is emitted by the induced adatom and reflected by the bump-plane interface. In the case of a rough surface,  $\gamma_s$  is given by<sup>11,12</sup>

$$\gamma_s = (2/\hbar) \text{Im}(F) , \quad (11)$$

where

$$F = \frac{1}{1 - \Gamma} \left[ \frac{(1 - \epsilon) \epsilon_0 Q_1'(\epsilon_1)}{\epsilon Q_1(\epsilon_0) - \epsilon_1 Q_1'(\epsilon_0)} + \Gamma \right] .$$

To include the effects of the laser bandwidth  $\gamma_L$ , the phase-diffusion model for the laser field has been used by defining the following correlation function for the Rabi frequency:

$$\langle\langle \Omega^-(t_1) \Omega^+(t_2) \rangle\rangle = \Omega^2 \exp(-\gamma_L |t_2 - t_1|) , \quad (12)$$

where the double bracket signifies two averages: one is over the stochastic ensemble and the other is a quantum mechanical average.

In the weak-field or large-detuning cases, where  $W(t) = \langle\langle \hat{W}(t) \rangle\rangle = -1$ , the population inversion of the two-level adatom has the following analytical form (for  $t \geq 0$ ):

$$\begin{aligned} W(t) = -1 + \Omega^2 \left\{ \frac{\tilde{\gamma}_2 + \gamma_L}{\gamma_1 [(\tilde{\gamma}_2 + \gamma_L)^2 + \Delta^2]} + \frac{\gamma_1 - \tilde{\gamma}_2 - \gamma_L}{\gamma_1 [(\gamma_1 - \tilde{\gamma}_2 - \gamma_L)^2 + \Delta^2]} \exp(-\gamma_1 t) \right. \\ \left. - \frac{[(\tilde{\gamma}_2 + \gamma_L)(\gamma_1 - \tilde{\gamma}_2 - \gamma_L) + \Delta^2] \cos(\Delta t) + \Delta(2\tilde{\gamma}_2 - 2\gamma_L - \gamma_1) \sin(\Delta t)}{[(\tilde{\gamma}_2 + \gamma_L)^2 + \Delta^2][(\gamma_1 - \tilde{\gamma}_2 - \gamma_L)^2 + \Delta^2]} \right. \\ \left. \times \exp[-(\tilde{\gamma}_2 + \gamma_L)t] \right\} . \quad (13) \end{aligned}$$

The corresponding power spectrum  $S(\omega)$  for the scattered light of the laser can be calculated through the Fourier transform of the dipole-dipole correlation function  $\langle\langle \hat{S}_{21}(t_2) \hat{S}_{12}(t_1) \rangle\rangle$ :

$$\begin{aligned}
S(\omega) = & \frac{\Omega^2}{2} \frac{1}{(\tilde{\gamma}_2 + \gamma_L)^2 + \Delta^2} \left\{ \frac{1}{(\tilde{\gamma}_2 - \gamma_L)^2 + \Delta^2} \right. \\
& \times \left[ \frac{\gamma_L(\tilde{\gamma}_2^2 - \gamma_L^2 + \Delta^2) + 2\gamma_L \Delta(\omega - \omega_L)}{\gamma_L^2 + (\omega - \omega_L)^2} - \frac{\tilde{\gamma}_2(\tilde{\gamma}_2^2 - \gamma_L^2 + \Delta^2) + 2\gamma_L \Delta(\omega - \omega_{21})}{\tilde{\gamma}_2^2 + (\omega - \omega_{21})^2} \right] \\
& \left. + \frac{2(\tilde{\gamma}_2 + \gamma_L) \tilde{\gamma}_2}{\gamma_L[\tilde{\gamma}_2^2 + (\omega - \omega_{21})^2]} \right\}. \quad (14)
\end{aligned}$$

The spectrum of light scattering in Eq.(14) exhibits two spectral peaks which are strongly influenced by the resonance interaction between the adatom and the bump-flat surface system in Eq.(6). One peak is centered at  $\omega = \omega_L$ , which corresponds to elastic or Rayleigh scattering, and the other peak is near  $\omega = \omega_{21}$ , corresponding to inelastic scattering or fluorescence.

In another limit, i.e., the case of a very strong driving field, nonlinear scattering and multiphoton excitation processes can be as important as single-photon processes. The scattering light spectrum  $S(\omega)$  of the adatom at steady state can obtain by solving the SBE [Eq.(10)] to obtain the dipole-dipole correlation function. The result is

$$\begin{aligned}
S(\omega) = & \frac{\Omega^2}{\Delta^2 + \alpha\Omega^2} \left\{ \frac{\Delta^2 + \tilde{\gamma}_2}{\Delta^2 + \alpha\Omega^2} \delta(\omega - \Omega_L) \right. \\
& + \frac{\Omega^2[(2\alpha - 1)\Delta^2 + \alpha^2\Omega^2]}{(\Delta^2 + \Omega^2)(\Delta^2 + \alpha\Omega^2)} \left[ \frac{S_0/\pi}{(\omega - \omega_L)^2 + S_0^2} \right] \\
& + \frac{1}{2} \frac{(\Omega' - \Delta)[\alpha(\Omega' - \Delta) + \Delta]}{(\Delta^2 + \Omega^2)} \left[ \frac{S_{\pm}/\pi}{(\omega - \omega_L + \Omega')^2 + S_{\pm}^2} \right] \\
& \left. + \frac{1}{2} \frac{(\Omega' + \Delta)[\alpha(\Omega' + \Delta) - \Delta]}{(\Delta^2 + \Omega^2)} \left[ \frac{S_{\pm}/\pi}{(\omega - \omega_L - \Omega')^2 + S_{\pm}^2} \right] \right\}. \quad (15)
\end{aligned}$$

where the parameter  $\alpha$  is defined as

$$\alpha = \tilde{\gamma}_2 / 2\gamma_2 . \quad (16)$$

In Eq.(15), we have assumed zero laser bandwidth,  $\gamma_L = 0$ . The detuning parameter is defined as

$$\Omega' = \Delta + \Delta_s \quad (17)$$

where

$$\Delta_s = \Delta [1 + (\Omega/\Delta)^2]^{1/2} - 1 , \quad (18)$$

and the widths of the profiles are

$$S_0 = 2\gamma_2 \left( \frac{2\Omega^2 + \Delta^2}{\Omega^2 + \Delta^2} \right) \quad (19)$$

$$S_{\pm} = S_+ = S_- = \gamma_2 \left[ \frac{(1 + \alpha)\Omega + 2\alpha\Delta^2}{\Omega^2 + \Delta^2} \right] . \quad (20)$$

Eq.(15) was derived under the assumption of a very strong coherent laser field, i.e.,  $\Omega^2 + \Delta^2 \gg \tilde{\gamma}_2^2$ . The strong-field spectrum, Eq.(15), has three spectral peaks: the coherent and incoherent parts of the Rayleigh scattering centered at  $\omega = \omega_L$  and the two side bands centered at  $\omega = \omega_L \pm \Omega'$  due to a multiphoton process and fluorescence of the adatom, referred to as the three-photon fluorescence components, respectively.<sup>11</sup> We shall see in the next section how the resonance coupling between adatom and bump influences the strong-field three-peak spectrum.

### 3. Numerical Results

Using Eqs.(13), (14) and (15), which describe the excitation and relaxation behavior of a two-level atom near or adsorbed on a metal surface with roughness (a bump on a flat surface), we have evaluated numerically some typical cases for the rough surface-modified resonance fluorescence spectrum. In all the calculations, the laser photon energy is taken to be 2.75 eV.

Figure 2 displays the rough surface-induced phase-decay constant  $\gamma_s$  as a function of the semi-minor axis  $b$  of the surface protrusion, with the semi-major axis  $a$  for the surface protrusion fixed at 100 Å. There is a sharp resonance peak at  $b \approx 38$  Å, corresponding to a resonant excitation of plasmons in the bump which can strongly enhance adatom-bump interaction, through the reflected field at the atomic site. Figures 3(a) and (b) display the influence of the plasmon resonance in the bump on the adatomic population distribution. The time oscillations of the population will decrease as the semi-minor axis  $b$  of the spheroidal bump approaches the plasmon resonance  $b \approx 38$  Å [Fig. 3(b)], indicating that the enhancement of the adatom-bump coupling leads to more damping of the adatomic oscillator.

Figure 4 displays the resonance fluorescence spectrum in the weak-field driving case [Eq.(14)], consisting of the Rayleigh and fluorescence peaks. The former peak in our model is determined by the laser bandwidth  $\gamma_L$ . The latter peak (fluorescence) strongly depends on the adatom-bump distance and the resonance coupling between the adatom and the bump. When the detuning  $\Delta$  gets smaller and the semi-minor axis  $b$  of the bump spheroid reaches the plasmon resonance condition [see Fig. 4(b)], the two peaks will overlap, where the fluorescence peak is strongly broadened by resonant adatom-bump coupling. In this case, the height of the Rayleigh peak will depend on the atom-bump distance and parameter  $b$ .

Figure 5 displays the typical three-peak spectrum of the strong-field-driven adatom using the formula of Eq.(15). In Fig. 5(a) we can distinguish the Rayleigh (central) peak, the three-photon peak (left) and the fluorescence peak (right). In these pictures we have drawn just the profile of the incoherent component of the Rayleigh scattering, as the coherent component will not be broadened by the surface bump.

In the smaller detuning case, i.e., Fig. 5(a), the spectrum has a distinctive three-peak nature. In this case, the three-photon peak (left) has measurable height, which is almost comparable with the fluorescence peak. It is seen that the smaller the adatom-bump distance, the larger the broadening equally in the three spectral peaks, due to the enhancement of the adatom-bump coupling for smaller distances. In the larger detuning case, i.e., Fig. 5(b), the driving effect of the applied laser field is weaker due to the large detuning  $\Delta$ . The height of the three-photon peak is decreased and the three-peak spectrum is transformed to the weak-field two-peak structure. In this case, smaller adatom-surface distances still lead to larger broadening, as in the former case.

#### 4. Summary

A simple model has been developed to describe the influence of surface roughness on the dynamic behavior of a two-level adatom near a metal surface. Surface-dressed optical Bloch equations (SBE), which account for surface-reflected photons and the resonance interaction due to plasmon excitation in the metal protrusion, have been derived. Based on the SBE, the population distribution of the adatom and the power spectrum of the scattered light, as well as the surface-enhanced dephasing broadening of the atomic spectrum, have been evaluated. Collisions with foreign gas atoms and effects of the laser bandwidth can also be considered in our model. It is shown that the spectrum of scattered light, as well as the level population of the adatom, are strongly enhanced by the resonantly excitation of plasmons in the hemispheroid on the metal surface. The displayed surface enhancement for the adatom-bump system should be very useful in understanding the spectroscopy and chemistry associated with rough surface.

Acknowledgments

This research was supported by the Office of Naval Research and the Air Force Office of Scientific Research (AFSC), United States Air Force, under Contract F49620-86-C-009. The United States Government is authorized to reproduce and distribute reprints for governmental purposes notwithstanding any copyright notation hereon. We acknowledge stimulating discussion with Professor David Ronis.



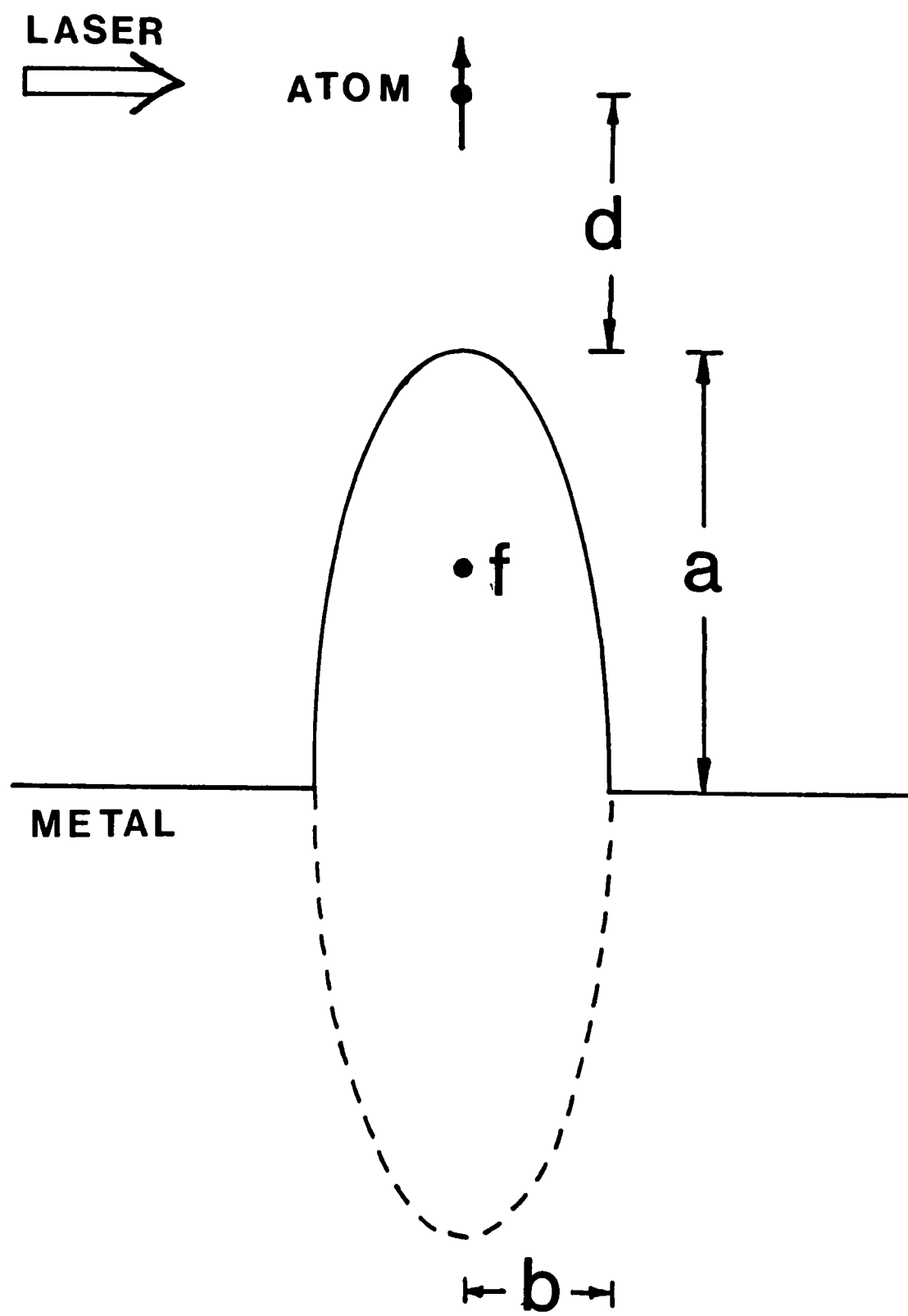
## References

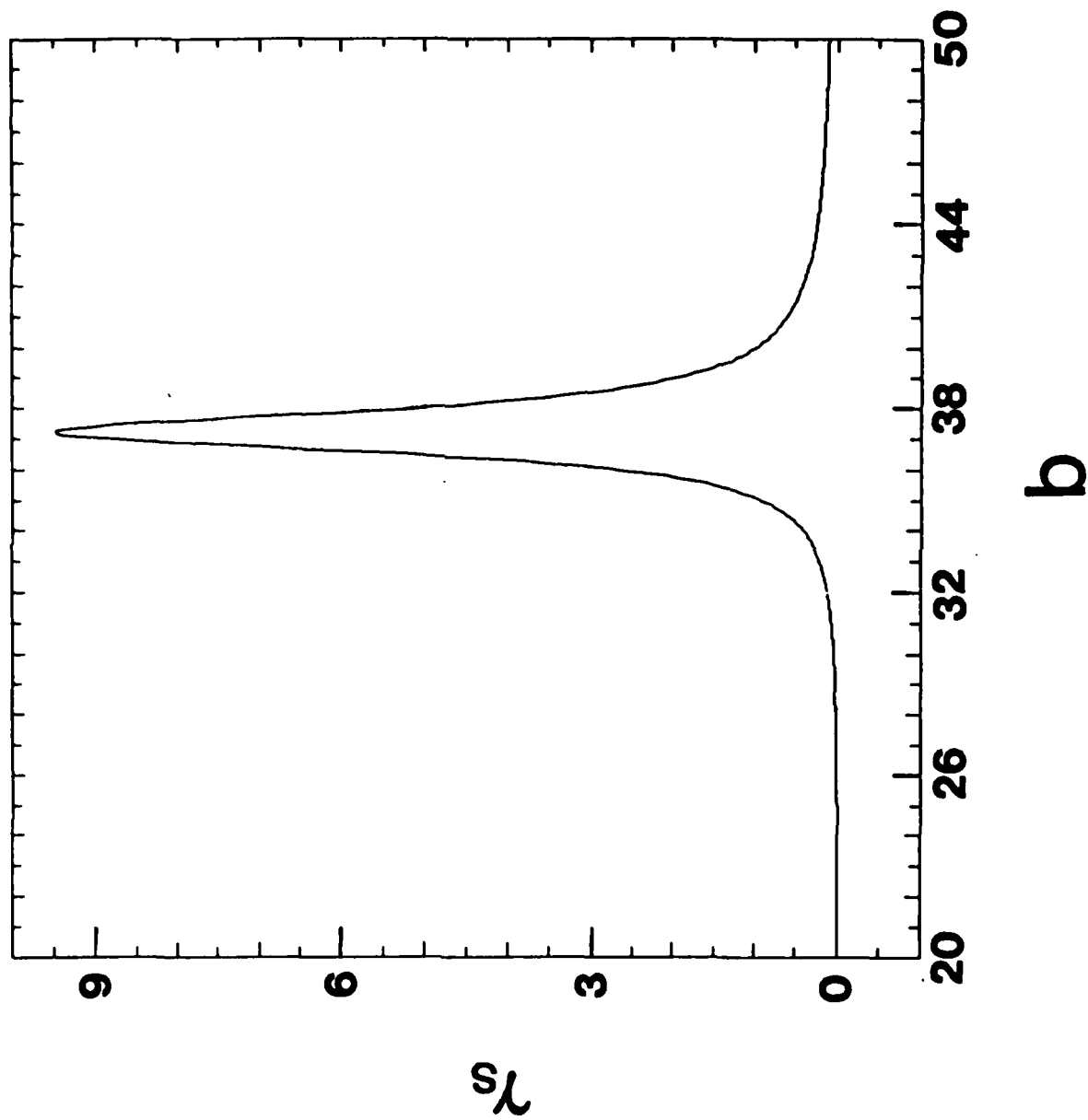
1. (a) For a comprehensive review, see Surface-Enhanced Raman Scattering, ed. by R. K. Chang and T. E. Furtak (Plenum, New York, 1982); (b) H. Metiu, *Prog. Surf. Sci.* 17, 153 (1984); (c) H. Metiu and P. Das, *Ann. Rev. Phys. Chem.* 35, 507 (1984); (d) M. Moscovitz, *Rev. Mol. Phys.* 57, 783 (1985).
2. V. L. Lyaboshitz, *Sov. Phys. JETP* 26, 937 (1968).
3. H. Morawitz, *Phys. Rev.* 187, 1972 (1969).
4. P. W. Milonni and P. L. Knight, *Opt. Commun.* 9, 119 (1973).
5. G. S. Agarwal, *Opt. Commun.* 42, 205 (1982).
6. R. Ruppin, *J. Chem. Phys.* 76, 1681 (1982).
7. P. Das and H. Metiu, *J. Phys. Chem.* 89, 4681 (1985).
8. D. A. Weitz, S. Garoff, J. I. Gersten and A. Nitzan, *J. Chem. Phys.* 78, 5324 (1983).
9. L. Allen and J. H. Eberly, Optical Resonance and Two-Level Atoms (Wiley, New York, 1975), pp. 28-78.
10. B. R. Mollow, *Phys. Rev.* 188, 1969 (1969).
11. X. Y. Huang, J. Lin and T. F. George, *J. Chem Phys.* 80, 893 (1984).
12. X. Y. Huang and T. F. George, *J. Phys. Chem.* 88, 4801 (1984).
13. X. Y. Huang, K. C. Liu and T. F. George, in Laser-Controlled Chemical Processing of Surfaces, ed. by A. W. Johnson, D. J. Ehrlich and H. R. Schlossberg (Elsevier, New York), *Mat. Res. Soc. Symp. Proc.* 29, 381 (1984).
14. X. Y. Huang, T. F. George and J. Lin, in Coherence and Quantum Optics V, ed. by L. Mandel and E. Wolf (Plenum, New York, 1984) pp. 685-693.
15. J. Lin, X. Y. Huang and T. F. George, *Solid State Commun.* 47, 63 (1983).
16. J. Gersten and A. Nitzan, *J. Chem. Phys.* 73, 3023 (1980).
17. A. C. Pineda and D. Ronis, *J. Chem. Phys.* 83, 5330 (1985).

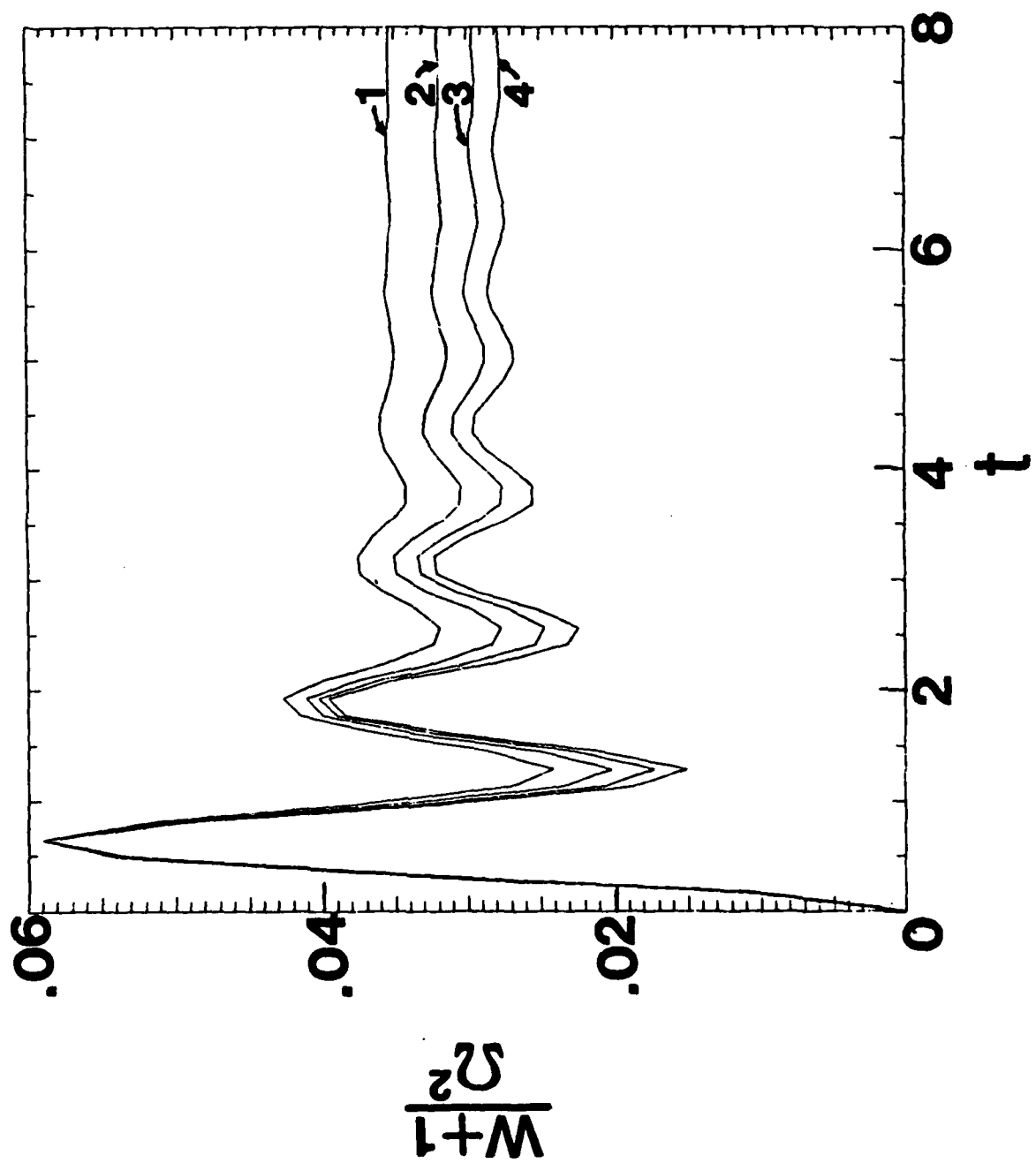
18. P. M. Morse and H. Feshbach, Methods of Theoretical Physics (McGraw-Hill, New York, 1953), p. 1284.
19. G. C. Schatz, in Surface-Enhanced Raman Scattering, ed. by R. K. Chang and T. E. Furtak (Plenum, New York, 1983), p. 35.

### Figure Captions

1. Geometry of the surface protusion. The semi-major axis is  $a$  and the semi-minor axis is  $b$ . The prolate spheroidal coordinates are defined by a scale factor,  $f$ , given by  $f = (a^2 - b^2)^{1/2}$ .
2. Rough surface induced phase-decay constant  $\gamma_s$  as a function of the semi-minor axis  $b$  of the surface protusion, where the semi-major axis is fixed at 100 Å.  $\gamma_s$  is in the unit of Einstein's spontaneous decay constant  $A$ .
3. Time evolution of the population inversion in the weak-field or large-detuning limit with  $(\gamma_L, \Omega, \Delta) = (0.3, 0.05, 5)$  in the unit of Einstein's spontaneous decay constant  $A$  for  $b = 34$  Å [Fig. 3(a)] and  $b = 38$  Å [Fig. 3(b)], with  $a$  fixed at 100 Å. The horizontal axis corresponds to time in the unit  $A^{-1}$ . The quantity  $[\omega(t) + 1]/\Omega^2$  is shown along the vertical axis. The curves numbered 1, 2, 3 and 4 correspond to the reduced atom-bump distance  $\bar{d} = 20, 25, 30$  and 35, respectively ( $\bar{d} = 2\pi d/\lambda$ , where  $\lambda$  is the laser wavelength).
4. Resonance fluorescence power spectrum of scattered light with  $(\gamma_L, \Omega, \Delta) = (0.3, 0.05, 5)$  in the unit  $A$  for  $b = 40$  Å [Fig. 4(a)] and  $b = 38$  Å [Fig. 4(b)]. Curves 1, 2 and 3 correspond to the reduced atom-bump distances  $\bar{d} = 20, 25$  and 30, respectively.  $X$  denotes  $(\omega - \omega_L)/(\omega_{21} - \omega_L)$  on the horizontal axis. The units along the vertical axis are arbitrary.
5. Strong-field surface-modified resonance fluorescence spectrum, where just the incoherent component of Rayleigh scattering is included, with  $(\Delta, \Omega, b) = (1, 10, 38)$  for Fig. 5(a) and  $(\Delta, \Omega, b) = (10, 10, 38)$  for Fig. 5(b).  $\Delta$  and  $\Omega$  are in the unit of  $A$  and  $b$  is in the unit Å. Curves 1, 2 and 3 correspond to the reduced atom-bump distances  $\bar{d} = 20, 25$  and 30, respectively.  $X$  denotes  $(\omega - \omega_L)/\Omega'$  on the horizontal axis. The units along the vertical axis are arbitrary.







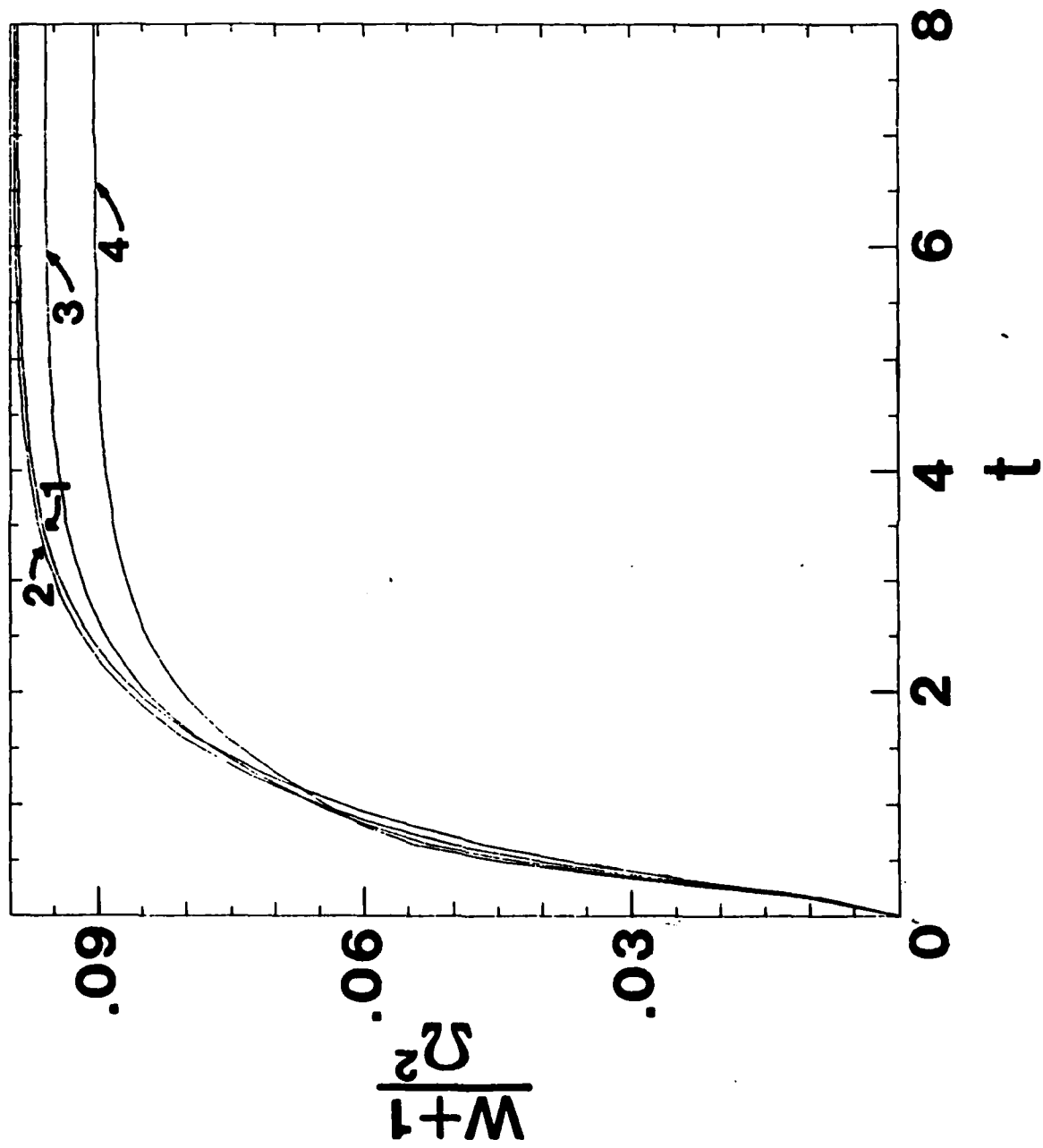
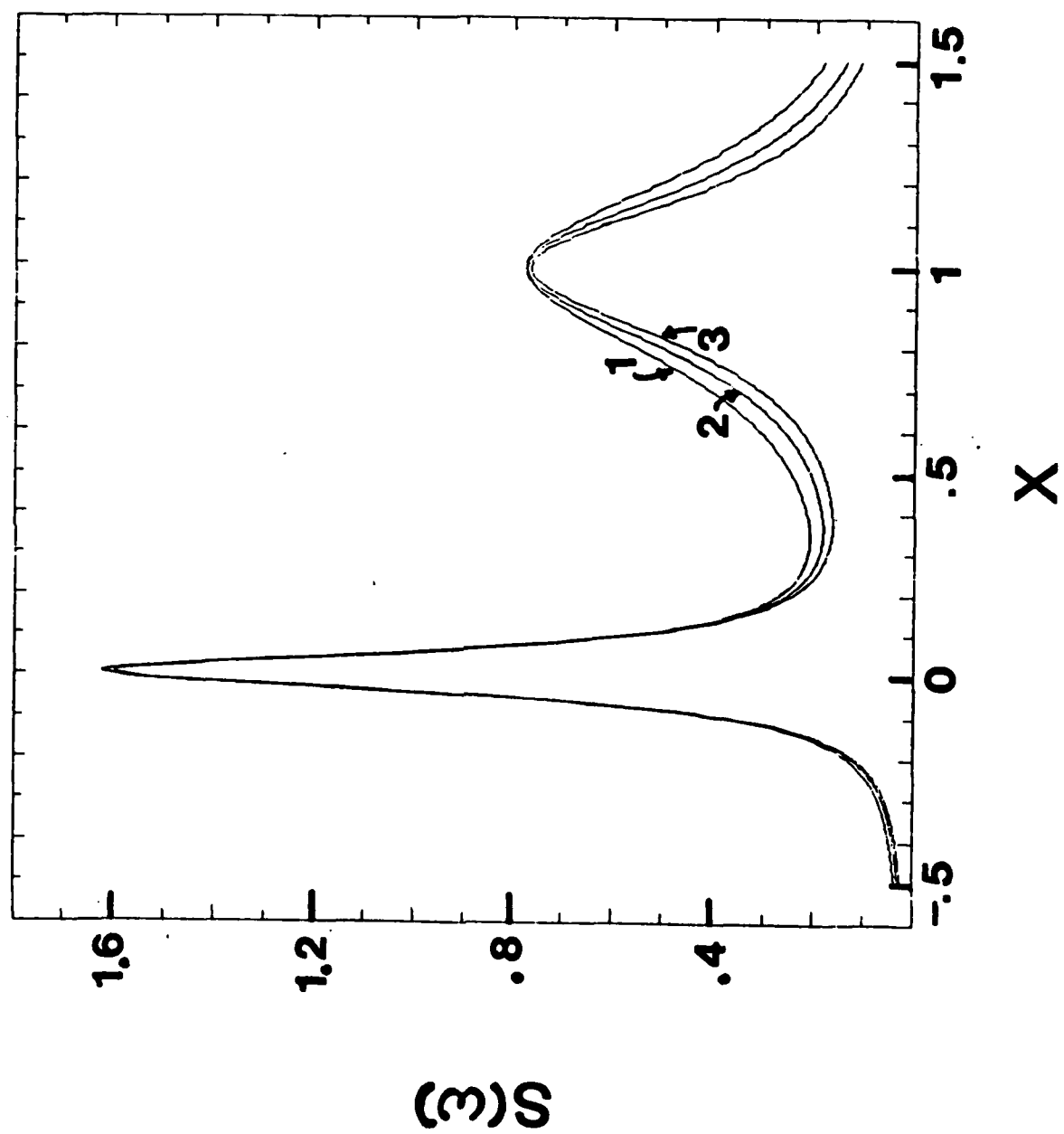
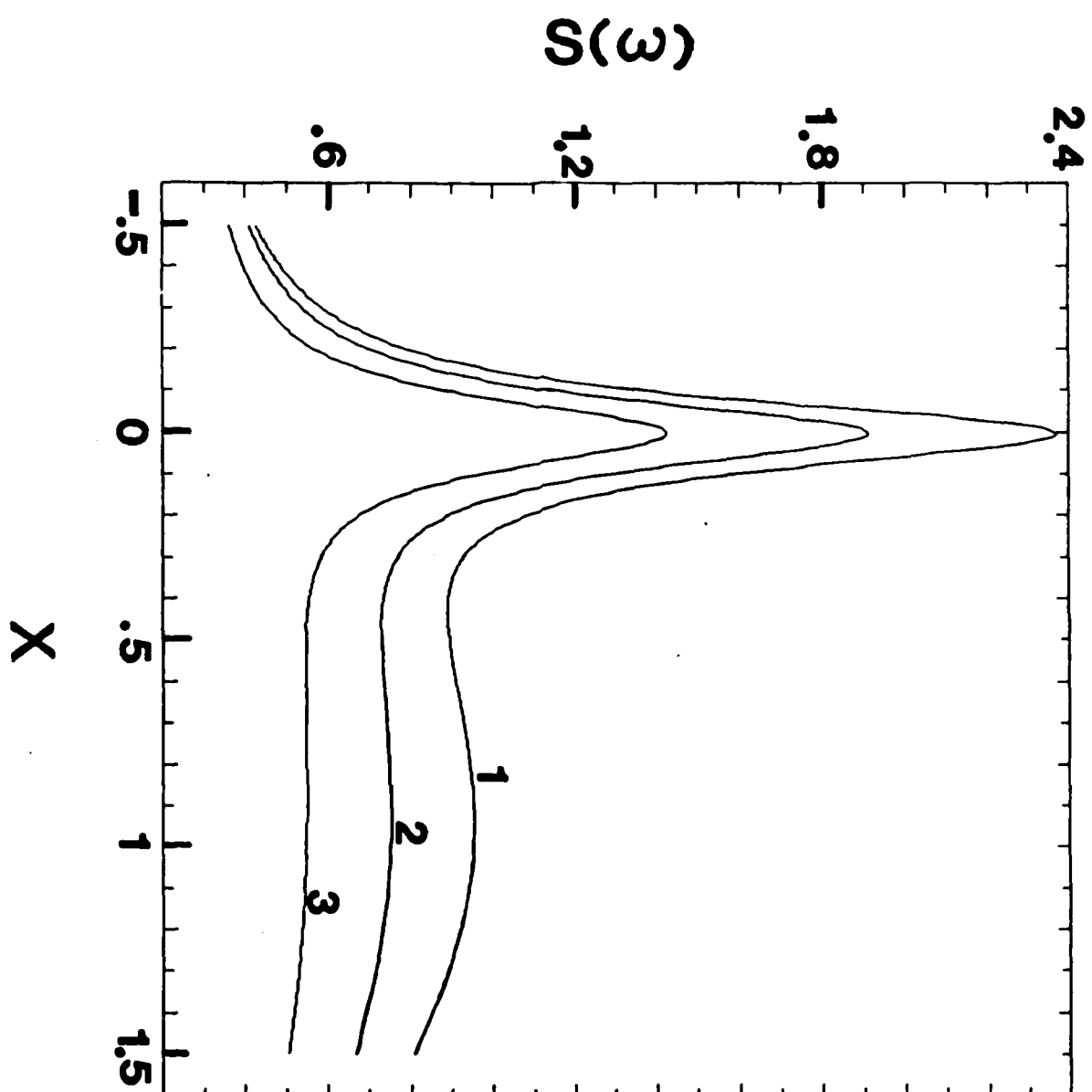


Fig. 3 - (b)







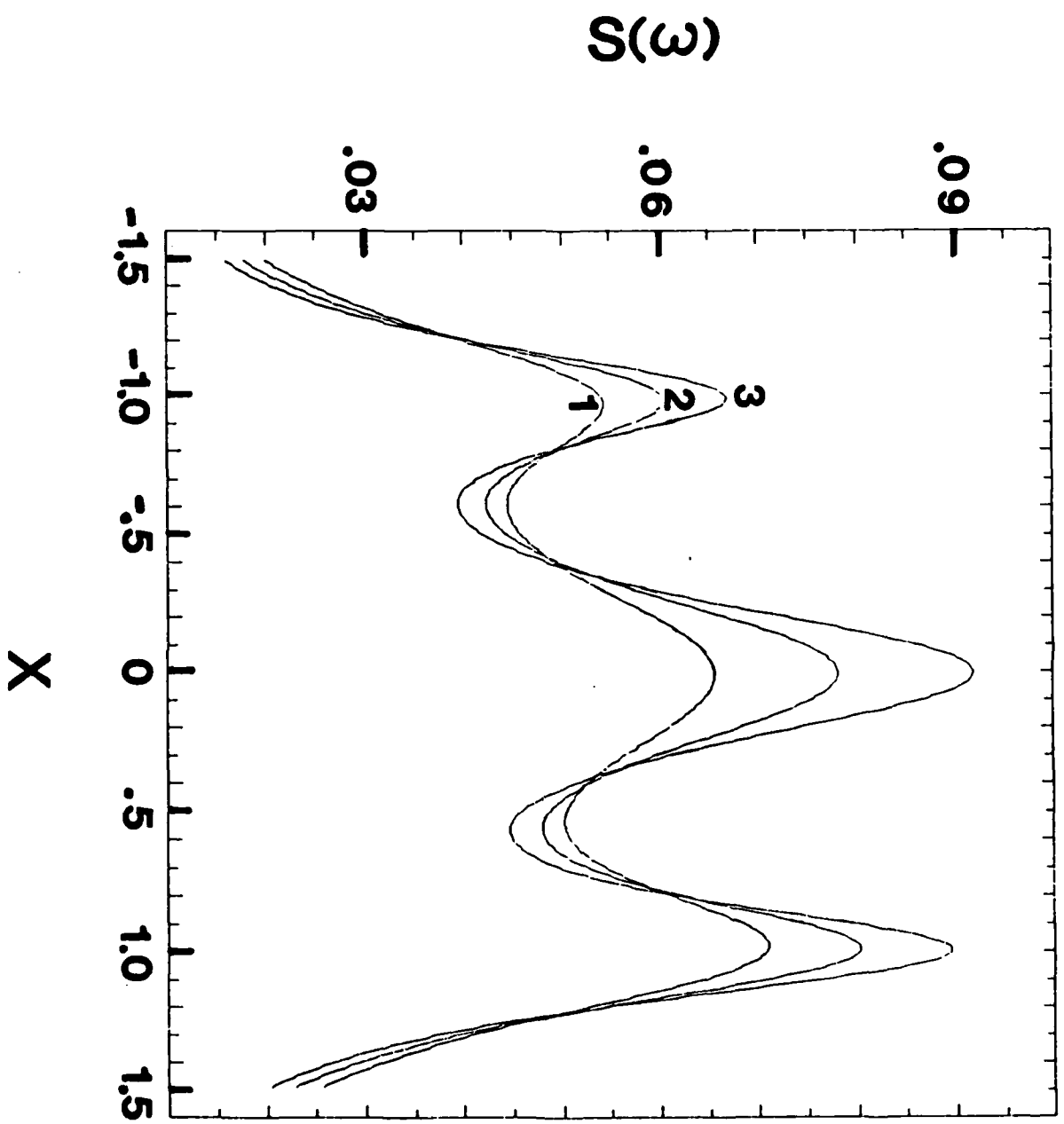
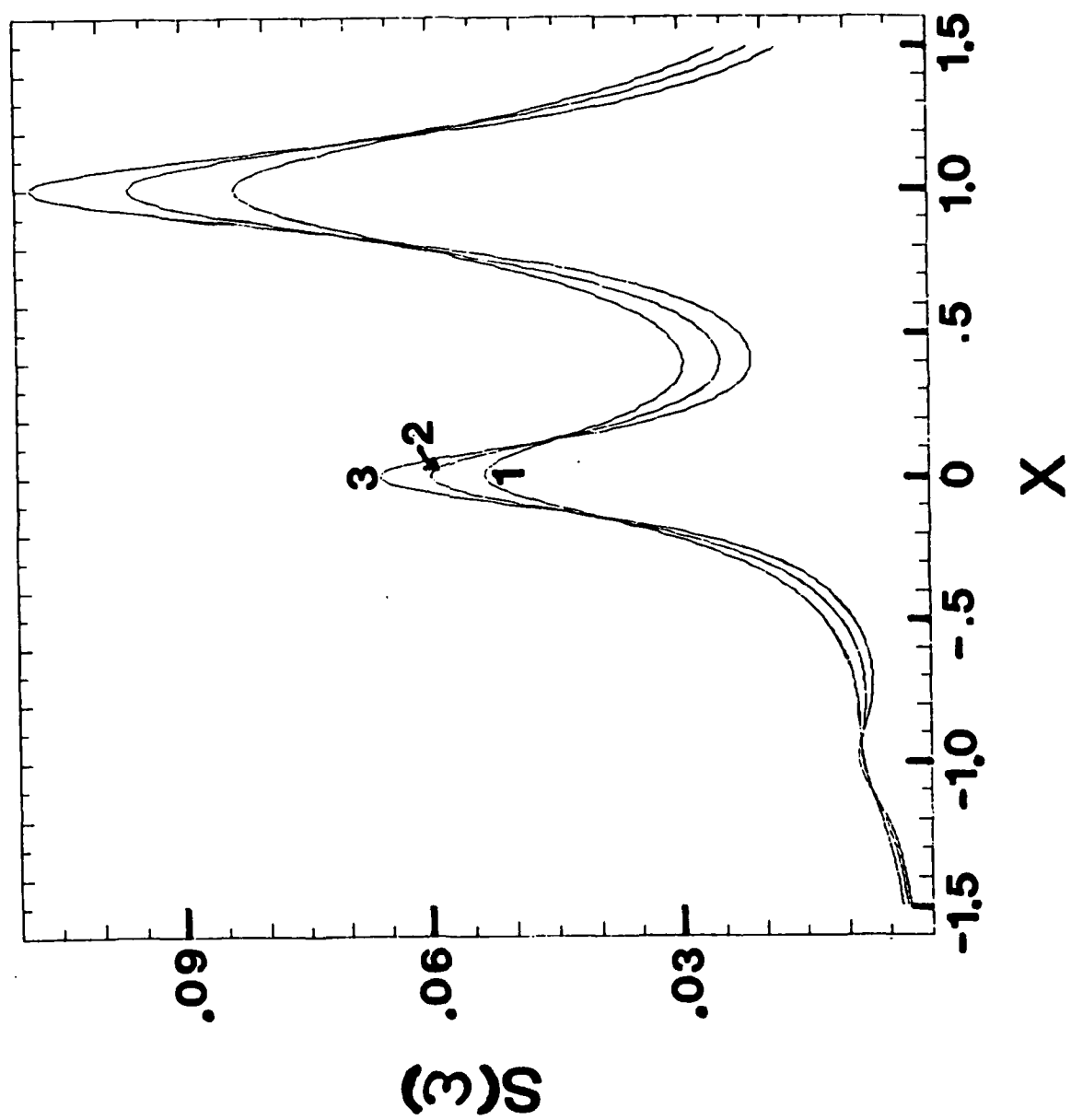


Fig. 5 (a)





T. George ONR Technical Report Mailing List - 10/19/84

Office of Naval Research  
Attn: Code 413  
800 N. Quincy Street  
Arlington, Virginia 22217

Dr. Bernard Douda  
Naval Weapons Support Center  
Code 5042  
Crane, Indiana 47522

Defense Technical Information Center  
Building 5, Cameron Station  
Alexandria, Virginia 22314

Commander, Naval Air Systems  
Command  
Attn: Code 310C (H. Rosenwasser)  
Washington, D.C. 20360

Dr. William Tolles  
Superintendent  
Chemistry Division, Code 6100  
Naval Research Laboratory  
Washington, D.C. 20375

Naval Civil Engineering Laboratory  
Attn: Dr. R. W. Drisko  
Port Hueneme, California 93401

Dr. David L. Nelson  
Chemistry Division  
Office of Naval Research  
800 North Quincy Street  
Arlington, Virginia 22217

DTNSRDC  
Attn: Dr. G. Bosmajian  
Applied Chemistry Division  
Annapolis, Maryland 21401

Dr. J. Murday  
Naval Research Laboratory  
Surface Chemistry Division (6170)  
455 Overlook Avenue, S.W.  
Washington, D.C. 20375

Dr. David Young  
Code 334  
NORDA  
NSTL, Mississippi 39529

T. George ONR Technical Report Mailing List - 10/19/84

Naval Weapons Center  
Attn: Dr. Ron Atkins  
Chemistry Division  
China Lake, California 93555

Dr. G. A. Somorjai  
Department of Chemistry  
University of California  
Berkeley, California 94720

Scientific Advisor  
Commandant of the Marine Corps  
Code RD-1  
Washington, D.C. 20380

Dr. J. B. Hudson  
Materials Division  
Rensselaer Polytechnic Institute  
Troy, New York 12181

U.S. Army Research Office  
Attn: CRD-AA-IP  
P.O. Box 12211  
Research Triangle Park, NC 27709

Dr. Theodore E. Madey  
Surface Chemistry Section  
Department of Commerce  
National Bureau of Standards  
Washington, D.C. 20234

Mr. John Boyle  
Materials Branch  
Naval Ship Engineering Center  
Philadelphia, Pennsylvania 19112

Dr. J. E. Demuth  
IBM Corporation  
Thomas J. Watson Research Center  
P.O. Box 218  
Yorktown Heights, New York 10598

Naval Ocean Systems Center  
Attn: Dr. S. Yamamoto  
Marine Sciences Division  
San Diego, California 91232

Dr. M. G. Lagally  
Department of Metallurgical  
and Mining Engineering  
University of Wisconsin  
Madison, Wisconsin 53706

T. George ONR Technical Report Mailing List - 10/19/84

Dr. R. P. Van Duyne  
Department of Chemistry  
Northwestern University  
Evanston, Illinois 60201

Dr. W. T. Peria  
Electrical Engineering Department  
University of Minnesota  
Minneapolis, Minnesota 55455

Dr. J. M. White  
Department of Chemistry  
University of Texas  
Austin, Texas 78712

Dr. Keith H. Johnson  
Department of Metallurgy  
and Materials Science  
Massachusetts Institute of Technology  
Cambridge, Massachusetts 02139

Dr. D. E. Harrison  
Department of Physics  
Naval Postgraduate School  
Monterey, California 93940

Dr. S. Sibener  
Department of Chemistry  
James Franck Institute  
5640 Ellis Avenue  
Chicago, Illinois 60637

Dr. W. Kohn  
Department of Physics  
University of California, San Diego  
La Jolla, California 92037

Dr. Arnold Green  
Quantum Surface Dynamics Branch  
Code 3817  
Naval Weapons Center  
China Lake, California 93555

Dr. R. L. Park  
Director  
Center of Materials Research  
University of Maryland  
College Park, Maryland 20742

Dr. A. Wold  
Department of Chemistry  
Brown University  
Providence, Rhode Island 02912

T. George ONR Technical Report Mailing List - 10/19/84

Dr. S. L. Bernasek  
Department of Chemistry  
Princeton University  
Princeton, New Jersey 08544

Dr. R. Stanley Williams  
Department of Chemistry  
University of California  
Los Angeles, California 90024

Dr. P. Lund  
Department of Chemistry  
Howard University  
Washington, D.C. 20059

Dr. R. P. Messmer  
Materials Characterization Lab  
General Electric Company  
Schenectady, New York 12301

Dr. F. Carter  
Code 6132  
Naval Research Laboratory  
Washington, D.C. 20375

Dr. Robert Gomer  
Department of Chemistry  
James Franck Institute  
5640 Ellis Avenue  
Chicago, Illinois 60637

Dr. Richard Colton  
Code 6112  
Naval Research Laboratory  
Washington, D.C. 20375

Dr. Ronald Lee  
R301  
Naval Surface Weapons Center  
White Oak  
Silver Spring, Maryland 20910

Dr. Dan Pierce  
Optical Physics Division  
National Bureau of Standards  
Washington, D.C. 20234

Dr. Paul Schoen  
Code 5570  
Naval Research Laboratory  
Washington, D.C. 20375



T. George ONR Technical Report Mailing List - 10/19/84

Dr. R. G. Wallis  
Department of Physics  
University of California  
Irvine, California 92717

Dr. J. T. Keiser  
Department of Chemistry  
University of Richmond  
Richmond, Virginia 23173

Dr. D. Ramaker  
Department of Chemistry  
George Washington University  
Washington, D.C. 20052

Dr. Roald Hoffman  
Department of Chemistry  
Cornell University  
Ithaca, New York 14853

Dr. J. C. Hemminger  
Department of Chemistry  
University of California  
Irvine, California 92717

Dr. R. W. Plummer  
Department of Physics  
University of Pennsylvania  
Philadelphia, Pennsylvania 19104

Dr. G. Rubloff  
IBM  
Thomas J. Watson Research Center  
P.O. Box 218  
Yorktown Heights, New York 10598

Dr. E. Yeager  
Department of Chemistry  
Case Western Reserve University  
Cleveland, Ohio 41106

Dr. Horia Metiu  
Department of Chemistry  
University of California  
Santa Barbara, California 93106

Dr. N. Winograd  
Department of Chemistry  
Pennsylvania State University  
University Park, Pennsylvania 16802

T. George ONR Technical Report Mailing List - 10/19/84

Dr. John T. Yates  
Department of Chemistry  
University of Pittsburgh  
Pittsburgh, Pennsylvania 15260

Dr. Adam Heller  
Bell Laboratories  
Murray Hill, New Jersey 07974

Dr. Richard Greene  
Code 5230  
Naval Research Laboratory  
Washington, D.C. 20375

Dr. Martin Fleischmann  
Department of Chemistry  
Southampton University  
Southampton SO9 5NH  
Hampshire, England

Dr. L. Kesmodel  
Department of Physics  
Indiana University  
Bloomington, Indiana 47403

Dr. John W. Wilkins  
Laboratory of Atomic and  
Solid State Physics  
Cornell University  
Ithaca, New York 14853

Dr. K. C. Janda  
California Institute of Technology  
Division of Chemistry and  
Chemical Engineering  
Pasadena, California 91125

Dr. Richard Smardzewski  
Code 6130  
Naval Research Laboratory  
Washington, D. C. 20375

Dr. E. A. Irene  
Department of Chemistry  
University of North Carolina  
Chapel Hill, North Carolina 27514

Dr. H. Tachikawa  
Department of Chemistry  
Jackson State University  
Jackson, Mississippi 39217

T. George ONR Technical Report Mailing List - 10/19/84

Dr. A. Steckl  
Department of Electrical and  
Systems Engineering  
Rensselaer Polytechnic Institute  
Troy, New York 12181

Dr. J. E. Jensen  
Hughes Research Laboratory  
3011 Malibu Canyon Road  
Malibu, California 90265

Dr. G. H. Morrison  
Department of Chemistry  
Cornell University  
Ithaca, New York 14853

Dr. J. H. Weaver  
Department of Chemical Engineering  
and Materials Science  
University of Minnesota  
Minneapolis, Minnesota 55455

Dr. P. Hansma  
Department of Physics  
University of California  
Santa Barbara, California 93106

Dr. W. Knauer  
Hughes Research Laboratory  
3011 Malibu Canyon Road  
Malibu, California 90265

Dr. J. Baldeschwieler  
Division of Chemistry  
California Institute of Technology  
Pasadena, California 91125

Dr. C. B. Harris  
Department of Chemistry  
University of California  
Berkeley, California 94720

Dr. W. Goddard  
Division of Chemistry  
California Institute of Technology  
Pasadena, California 91125

Dr. A. Reisman  
Microelectronics Center  
of North Carolina  
Research Triangle Park  
North Carolina 04469

T. George ONR Technical Report Mailing List - 10/19/84

Dr. M. Grunze  
Laboratory for Surface Science  
and Technology  
University of Maine  
Orono, Maine 04469

Dr. F. Kutzler  
Department of Chemistry  
Box 5055  
Tennessee Technological University  
Cookeville, Tennessee 38501

Dr. J. Butler  
Naval Research Laboratory  
Code 6115  
Washington DC 20375

Dr. D. DiLella  
Chemistry Department  
George Washington University  
Washington DC 20052

Dr. L. Interante  
Chemistry Department  
Rensselaer Polytechnic Institute  
Troy, New York 12181

Dr. R. Reeves  
Chemistry Department  
Rensselaer Polytechnic Institute  
Troy NY 12181

Dr. Irvin Heard  
Chemistry and Physics Department  
Lincoln University  
Lincoln University, Pennsylvania 19352

Dr. David young  
Code 334  
NORDA  
NSTL, Mississippi 39529

Dr. K. J. Klaubunde  
Department of Chemistry  
Kansas State University  
Manhattan, Kansas 66506

END

FILMED

2-86

DTIC